JOC The Journal of Organic Chemistry

Article

pubs.acs.org/joc

Atropisomerism in Tertiary Biaryl 2-Amides: A Study of Ar−CO and Ar−Ar′ Rotational Barriers

Marianne Lorentzen,[†] Indrek Kalvet,[‡,§,∥] Francoise Sauriol,[∥] Toni Rantanen,[‡,∥] Kåre B. Jørgensen,*[,†] and Victor Snieckus*[,‡,∥]

[†]Faculty of Science and Technology, University of Stavanger, N-4036 Stavanger, Norway

[‡]Snieckus Innovations, Queen's University, Kingston, ON K7L 3N6, Canada

[§]Institute of Chemistry, University of Tartu, Ravila 14A, 50411 Tartu, Estonia

[∥]Department of Chemistry, Queen's University, 90 Bader Lane, Kingston, ON K7L 3N6, Canada

Supporting Information

ABSTRACT: A rotational barrier study was performed on eight tertiary biaryl 2-amides using variable-temperature (VT) NMR and exchange (EXSY) spectroscopy experiments. Seven out of the eight 2-amido-2′-methylbiphenyls with additional 3- and 6-substitution patterns (**1**−**7**) were found to have approximately similar rotational barriers ($\Delta G^{\ddagger}_{Tc}$ = 56.5−67.5 kJ/mol). However, for both 3- and 6-substitution (**8**), the rotational barrier was found to be significantly higher ($\Delta G^{\ddagger}$ = 102.6−103.8 kJ/mol). Computational studies performed on all eight compounds gave results in good agreement with the experimental rotational barriers. A transition state in which atropisomerism occurs by a cooperative rotation of the Ar−CO and Ar−Ar′ bonds depending on substituent location is proposed.

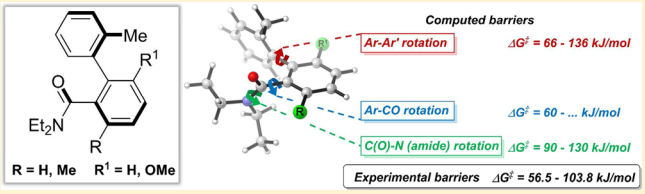

INTRODUCTION

Atropisomeric molecules, discovered by Christie and Kenner[1] in 1922, exhibit restricted rotation (torsion) around a single bond due to excessive nonbonded interactions.[2] Atropisomerism is predominantly associated with biaryls[3] and binaphthyl,[4] in which pivotal bond rotation is prevented by bulky substituents, thus allowing the isolation of enantiomeric forms. This type of molecular chirality has had considerable significance in the development of chiral auxiliaries and ligands for asymmetric synthesis.[5] Furthermore, since many biologically active biaryl compounds possess chirality due to restricted rotation,[6] atropisomerism has become important in drug discovery endeavors.[7] Tertiary aryl amides and anilides, known to display atropisomerism,[8] allow generation of atropisomers directly[9] or by dynamic kinetic resolution.[10] These compounds have also been used as effective chiral ligands[11] and auxiliaries.[12] In particular, aryl amides, well-known to have high rotational barriers due to the partial double bond character of the C−N bond arising from amide bond resonance,[13] have been shown to exhibit rotational barriers from cooperative C−N/Ar−CO rotations by the elegant and extensive investigations of Clayden and co-workers.[14]

In the course of recent studies, we prepared a series of 2-amido-2′-methyl biaryls (Figure 1) for the development of a general route to phenanthrenes[15,16] and noted that this biaryl structure type has three bonds that may give rise to high rotational barriers, the CO−N (amide) bond (green), the Ar−CO bond (blue), and the Ar−Ar′ (biaryl) bond (red), and hence may be amenable to a rotational barrier investigation by VT NMR spectroscopy.

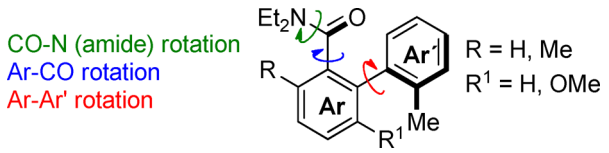

Figure 1. Potential rotational barriers of 2-amido-2′-methylbiaryls.

Herein, we report a rotational barrier study of a series of substituted 2-amido-2′-methylbiaryls (**1**, **4**−**8**), a 2-(2′-methylphenyl)naphthamide (**2**), and a 2-(1′-methyl-2′-naphthyl)benzamide (**3**) (Figure 2). Thus, three substrates with no other substituents but with variation of phenyl to naphthalene rings (**1**−**3**), three biaryl 2-amides with additional substituents, 6,3′- (**4**), 6- (**5**), 6,5′- (**6**), and 3,5- (**7**), and one biaryl with a 3,6,2′-substitution pattern (**8**) were investigated. On the basis of previous studies concerning the rotational barriers of substituted biaryls,[3] observation of high Ar−Ar′ rotational barriers was expected for compounds **4**−**6** and **8**.

In the course of studies concerned with the preparation of chrysenols (Scheme 1), we observed that treatment of something incorporating naphthyl, such as 2'-methyl-2-amidonaphthyl **2** under excess LDA conditions resulted in directed remote metalation (DreM)−cyclization to afford 5-chrysenol **9** (Scheme 1).[15d,16] However, in some cases,[15d,16]

Received: April 13, 2017
Published: June 22, 2017

DOI: 10.1021/acs.joc.7b00890
J. Org. Chem. 2017, 82, 7300−7308

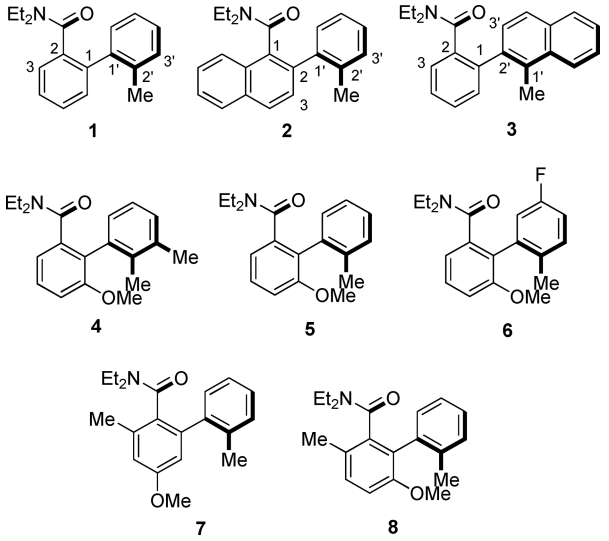

Figure 2. 2-Amidobiaryls in the present rotational barrier study. IUPAC numbering is given. Biaryls **4**–**8** follow the numbering of biaryl **1**.

fluorenone derivatives were formed, e.g., the conversion of **3** into fluorenone **10** instead of the 6-chrysenol **11**. The ^{1}H NMR spectra of biaryls **2** and **3** displayed evidence for the presence of two rotamers/diastereomers, strongly suggesting, as one rationalization, a high kinetic barrier due to hindered rotation about the biaryl bond which prevents attainment of the necessary transition state for the DreM reaction.[17] As a precedent for this supposition, we have previously observed a case where, of two isolated atropisomers, only one underwent a DreM reaction.[18] These results enhanced further our interest in the present investigation.

RESULTS AND DISCUSSION

All compounds were prepared either by the directed *ortho*-metalation (DoM)–boronation reactions of *N*,*N*-diethyl benzamides, followed by Suzuki–Miyaura cross-coupling reactions of the resulting boronic acids with 2-bromotoluenes, or by reaction of the reversed coupling partners.[16] For the VT ^{1}H NMR experiments, all compounds, with the exception of compounds **2** (23 °C, 298 K) and **3** (−83 °C, 190 K), were cooled to 250 K before ^{1}H NMR, NOESY, and COSY measurements were recorded. At these low temperatures, the maximum chemical shift differences ($\Delta\nu$ in Hz) between the two exchanging 2′-methyl peaks were obtained. The rate constant, k_c of the interconversion of the two exchanging rotamers at coalescence temperature, T_c, was estimated by the Gutowsky–Holm equation.[19] From the coalescence temperature, T_c, and the rate constant, k_c, the activation energy of rotation ($\Delta G^{\ddagger}_{Tc}$) was calculated using the Eyring equation[20] (see the SI).

For compounds **2** and **5** as illustrative cases, the VT ^{1}H NMR data are depicted in Figure 3. At low temperature (298 and 250 K for compounds **2** and **5**, respectively) the two exchanging 2′-methyl signals are observed as two singlets due to a slow exchange process. Raising the temperature resulted in the expected increased rate of exchange of the two rotamers, observed by broadening of the two signals and eventual coalescence. For substrate **2**, coalescence occurred at 332 K, while for substrate **5** it occurred at 314 K, which resulted in calculated rotational energy barriers of $\Delta G^{\ddagger}_{Tc}$ = 67.5 and 63.0 kJ/mol, respectively. The results of the VT ^{1}H NMR studies of the 2-amido-2′-methylbiaryls **1**–**7** are tabulated in Table 1. The 3-Me-6-OMe biaryl amide **8** had a very high energy barrier, and we were unable to approach the coalescence temperature, even at up to 380 K[21] in DMSO-d_6.

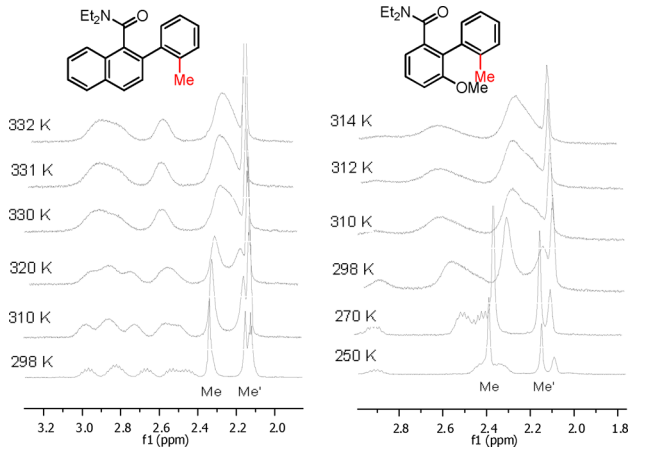

Figure 3. VT ^{1}H NMR of compounds **2** and **5**.

To interpret the VT-NMR data, one must consider that the possibility of both Ar–CO and Ar–Ar′ rotations leads to enantiotopic and diastereotopic rotamers (Figure 4).[14] Rotamers due to only Ar–CO rotation or Ar–Ar′ rotation will, due to the diastereotopic rotamer properties, show

Scheme 1. Selectivities of the DreM Cyclization of *o*-Arylnaphthamide 2 and Benzamide 3[a]

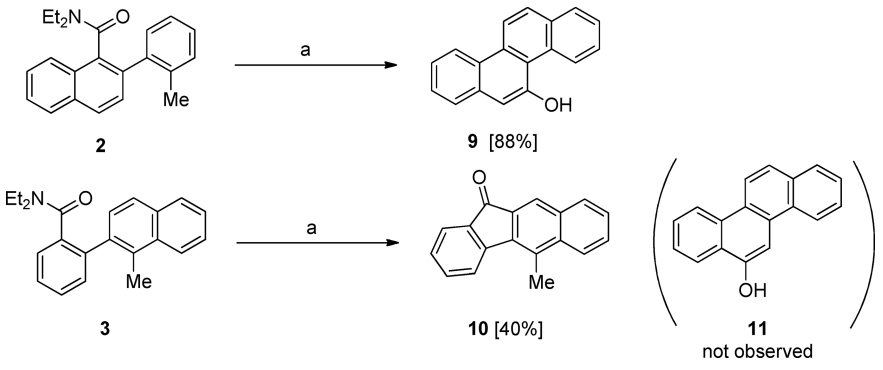

[a]Conditions: (a) LDA (2.5 equiv), THF, rt.

DOI: 10.1021/acs.joc.7b00890
J. Org. Chem. 2017, 82, 7300–7308

Table 1. Rotational Barriers of Compounds 1−7 from VT-NMR Measurements[a,b]

entry	compd	δ (ppm)	Δν[c] (Hz)	T_c (°C) (K)	k_c[d] (s^{-1})	$\Delta G^{\ddagger}_{Tc}$[e] (kJ/mol)
1	**1**	2.35, 2.08	106.9	11 (284)	237	56.5
2	**2**	2.30, 2.12	74.4	59 (332)	165	67.5
3	**3**	2.46, 2.35	42.8	10 (283)	95	58.5
4	**4**	2.26, 2.04	89.4	40 (313)	198	63.0
5	**5**	2.39, 2.15	96.6	41 (314)	214	63.0
6	**6**	2.24, 2.02	88.8	28 (301)	197	60.5
7	**7**	2.43, 2.13	117.1	52 (325)	260	64.8

[a]400 MHz NMR. [b]Lowest temperature reached: −83 °C (190 K). [c]Δν obtained from the methyl peak in exchange at low temperature. [d]k_c = 2.22Δν. [e]Estimated margin of error ±0.8 kJ/mol.

different distinct signals between atropdiastereomers **A** and **B** in the ^{1}H NMR spectra, which thereby also allow an EXSY-NMR study.[22] The **A**−**B** atropdiastereomeric exchange study of compound **8**, for which a coalescence temperature was unattainable, was carried out in toluene-d_8 at 380 K with mixing times from 1 to 0.01 s. The rotational barrier was calculated from the volume integrals of the exchange peaks (entry 9, Table 2). (For a complete discussion of these experiments, see the SI, section 2). To verify that these results could be compared with the variable-temperature experiments, the EXSY-NMR experiments were also conducted on compound **5** in acetone-d_6 at 273 K with mixing times from 1 to 0.003 s (entry 6, Table 2). That the rotational energy barrier is almost insensitive to solvents was demonstrated for compound **5** by experiments in toluene-d_8 and $CDCl_3$, which gave the same energy barrier within 1.4 kJ/mol. Atropdiastereomers **A** and **B** of compound **8** were separated by standard flash chromatography. The structure of atropdiastereomer **B** (Figure 4) was assigned by observation of an NOE between the 2′-methyl and the amide methylene protons (SI, section 2.6). Its isomerization to atropdiastereomer **A** at 232 K (SI, section 2.4) was studied by ^{1}H NMR and showed an energy barrier

Table 2. Calculated[a] **and Experimental (VT ^{1}H NMR) Rotational Barriers (in kJ/mol)**

Entry	Compound	Measured ($\Delta G^{\ddagger}_{Tc}$)	Ar-Ar′ ($\Delta G^{\ddagger}$)	Ar-CO ($\Delta G^{\ddagger}$)	Et_2N-CO (*syn*) ($\Delta G^{\ddagger}$)	Et_2N-CO (*anti*) ($\Delta G^{\ddagger}$)	Ar-CO / Et_2N-CO ($\Delta G^{\ddagger}$)
1	**1**	56.5	66.2	62.1	115.1	-	91.0[e]
2	**2**	67.5	68.0	-	124.3	105.2	109.5[f]
3	**3**	58.5	81.4	63.2	90.3	-	91.3[f]
4	**4**	63.0	135.6	68.9	112.7	-	93.1[e,f]
5	**5**	63.0	126.8	68.6	112.8	-	91.8[e,f]
6	**5**	63.6-64.5[b]					
7	**6**	60.5	123.0	60.5	109.0	-	84.5[e]
8	**7**	64.8	69.4	-	130.8	104.0	95.5[f]
9	**8**	102.6[c]	126.7	-	122.0 (B) 130.2 (A)	107.9 (B) 104.1 (A)	108.1[f]
10	**8**	103.8[d]					

[a]Calculations were performed at CPCM (toluene) M06L/6-311++G(d,p)//CPCM (toluene) ωB97XD/6-31+G(d) level of theory. [b]EXSY-NMR experiment in acetone-d_6 at 273 K (SI, section 2.3). [c]EXSY-NMR experiment in toluene-d_8 at 380 K (SI, section 2.2). [d]Isomerization of pure atropdiastereomer **8B** at 232 K (SI, section 2.4). [e]Ar′−O transition state. [f]Ar′−N transition state. "−": The transition state could not be located.

(entry 10, Table 2) that was in good agreement with that measured by EXSY-NMR.

As expected, biaryls without amide and biaryl axis-obstructing 3- and 6-substituents, **1** and **3**, respectively (entries 1 and 3, Table 1), showed the lowest rotational barriers. The 6-OMe bearing biaryls **4**, **5**, and **6** showed somewhat higher activation energies (entries 4, 5, and 6) but less enlarged than expected by a hindered biaryl rotation. Of the methods for assessing the steric bulk of substituents,[23] we compared our results with those for structurally related biaryl systems. In biaryl rotations,[27] the methoxy group has a smaller effective van der Waals radii (1.52 Å) than the methyl group (1.80 Å) but should still give a substantial increase in the rotational barrier as observed in the comparison of biaryls **12** with **13** (Figure 5a).[24] On the other hand, benzamide **16** (Figure 5c), which closely resembles **4**−**6**, shows a $\Delta G^{\ddagger}_{Tc}$ = 63.2 kJ/mol that must be attributed to the Ar−CO rotational barrier in view of the

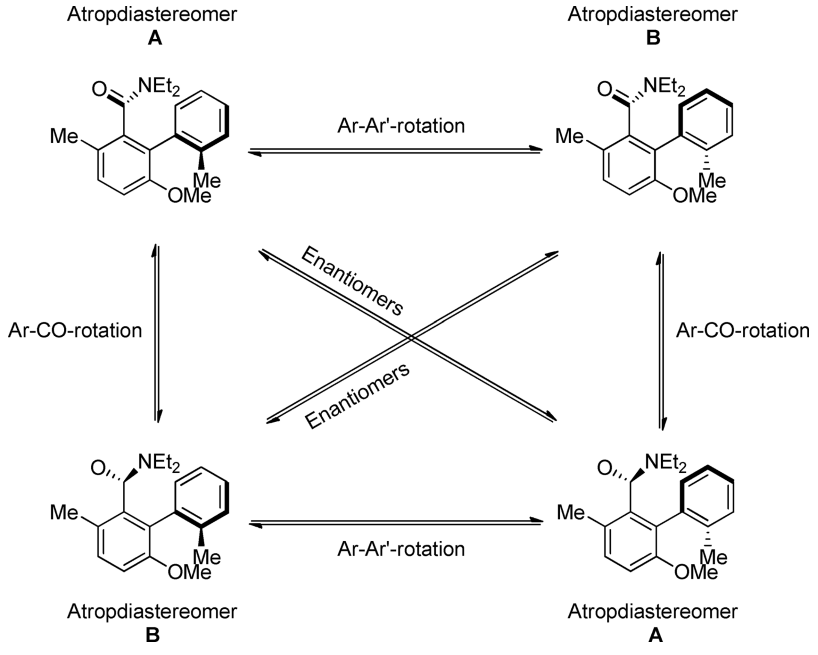

Figure 4. Diastereotopic and enantiotopic rotamers of biaryl amide **8** resulting from Ar−Ar′ and Ar−CO rotations.

DOI: 10.1021/acs.joc.7b00890
J. Org. Chem. 2017, 82, 7300−7308

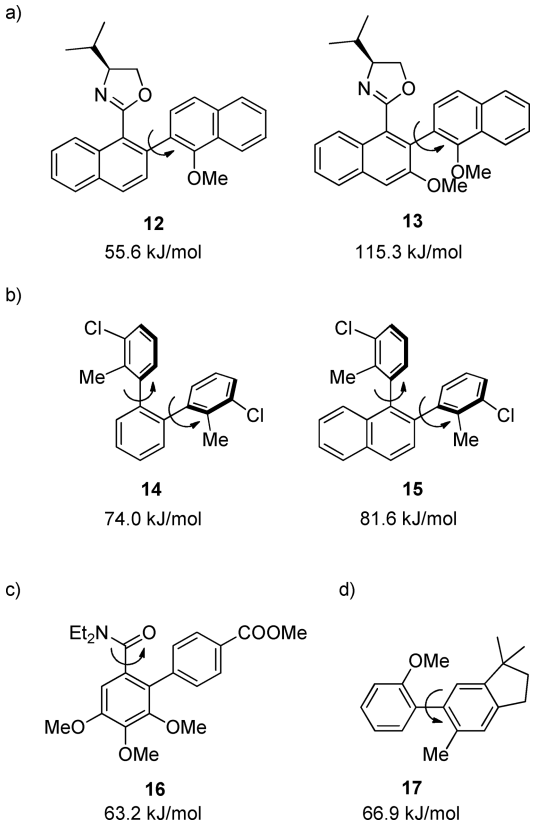

Figure 5. Rotational barriers for relevant biaryls: (a) effect of an OMe group on Ar−Ar rotation;[24] (b) *peri*-H effect;[3a] (c) isolated Ar−CO rotation;[25] (d) isolated Ar−Ar rotation.[27]

symmetry of the other aryl ring.[25] Consequently, the **A**−**B** diastereoisomer interconversions for biaryls **4**, **5**, and **6** occur through Ar−CO rotation. Furthermore, the additional 3′-Me substituent (**4**) had little or no effect. For comparison, although electronically different from **4**, a similarly positioned 3′-ethyl group in a 2,2′-bis(trifluoromethyl)biphenyl (not shown) provides an approximately 16 kJ/mol buttressing effect compared to the desethyl system.[26]

The 5′-F-substituted biaryl **6** showed a slightly lower activation energy than the nonfluorinated analogue **5** (compare entries 5 and 6). A higher rotational activation energy was found for naphthamide **2** (entry 2, $\Delta G^{\ddagger}_{Tc}$ = 67.5 kJ/mol), which corresponds to a 11.0 kJ/mol buttressing effect of the *peri*-hydrogen (C-8) in **2** compared to biaryl **1**. For comparison with these results, in an investigation of benzene and naphthalene systems (Figure 5b), compound **15** was shown to have a $\Delta G^{\ddagger}$ = 7.6 kJ/mol higher than that of compound **14**, which may be also attributed to a *peri*-hydrogen effect in the former compound.[3a] In our study, incorporation of a 3-methyl group as in **7** (entry 7, Table 1) results in a significantly higher activation energy ($\Delta\Delta G^{\ddagger}_{Tc}$= 8.3 kJ/mol) compared to that of the prototype **1** but slightly lower than that observed for the compound with a *peri*-hydrogen effect (**2**). Thus, these observations offer rationalization of both Ar−Ar′ and Ar−CO rotations. Compound **8** in which the Ar−CO rotation is hindered by the 3-Me substituent, while the Ar−Ar′ rotation is hindered by the 6-OMe substituent shows a much higher rotational barrier than that observed for other compounds lacking this double hindrance effect.

Our results of very similar $\Delta G^{\ddagger}_{Tc}$ values for the series of compounds **1**−**7** made it difficult to distinguish between the individual Ar−CO and Ar−Ar′ rotations in several studied cases. To shed more light on the dynamics of these molecules, a series of computational studies was performed.

COMPUTATIONAL STUDIES

A computational study at the CPCM (Toluene) M06L/6-311++G(d,p)//CPCM (toluene) ωB97XD/6-31+G(d) level of theory was undertaken to further understand the experimentally measured barriers for compounds **1**−**8**.[28] Five different bond rotations were considered: the biaryl bond (Ar−Ar′), the aryl−carbonyl bond (Ar−CO), the amide bond (Et_2N−CO, via *syn* and *anti* transition states), and a combined rotation of the Ar−CO bond and the amide bond[29] (Ar−CO/Et_2N-CO; *anti* TS only). The corresponding transition-state structures are depicted in Figure 6. All barriers are reported relative to the

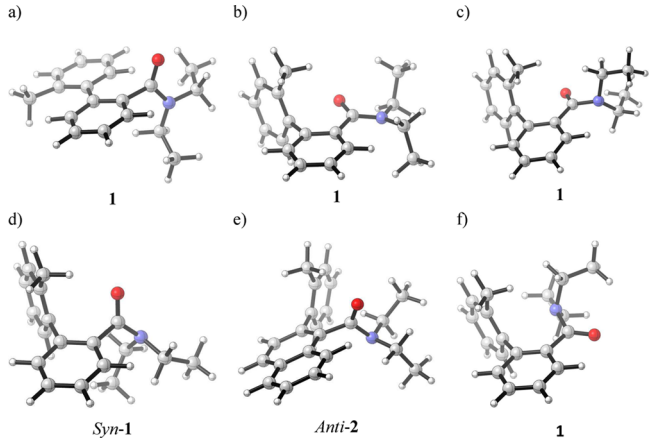

Figure 6. Calculated transition states for the different bond rotations of biaryl amides **1** and **2**. (a) Ar−Ar′ bond rotation, (b) Ar−CO bond rotation, (c) Ar−CO/Et_2N−CO combined rotation with Ar′ and O eclipsed in the transition state, (d) C=O−N bond rotation with *syn*-transition state, (e) C=O−N bond rotation with *anti*-transition state, (f) Ar−CO/Et_2N−CO combined rotation with Ar′ and N eclipsed in the transition state.

corresponding lowest energy atropisomer in kJ/mol. Table 2 shows the comparison of the results from the computational study with the corresponding experimentally determined values.

The DFT calculations suggest that for compounds **1**, **2**, and **4**−**8**, the atropdiastereomer **B** is on average $\Delta G_f^{\theta} \approx$ 1.3 kJ/mol lower in energy than **A**. (The exception, biaryl amide **3**, has atropdiastereomer **A** calculated to be ΔG_f^{θ} = 3.3 kJ/mol more stable.) These results concur with the EXSY-NMR experiments that show that the energy barriers of the **B**−**A** interconversions of **5** and **8** were slightly larger than those of the **A**−**B** interconversions (SI, sections 2.2 and 2.3). Studies of energy differences between atropdiastereomers in biaryl amides have been previously reported by Clayden.[30]

The DFT calculations for the Ar−Ar′ rotation give a $\Delta G^{\ddagger}$ = 66.2−69.4 kJ/mol range for molecules without a 6-substituent (Table 2, compounds **1**, **2**, and **7**). In the transition state of **1** (Figure 6a), the amide group is almost orthogonal to the biaryl plane and twisted away from the bond of rotation. This rotational barrier is comparable to that observed for biaryl **17** (Figure 5d), which bears only 2-methoxy and 2′-methyl substituents ($\Delta G^{\ddagger}$ = 66.7 kJ/mol).[27] For compound **3**,

DOI: 10.1021/acs.joc.7b00890
J. Org. Chem. 2017, 82, 7300−7308

involving an aryl−naphthyl rotational barrier (entry 3, Table 2), a slight buttressing effect may be responsible for the higher energy barrier as discussed in the section on the VT-NMR experiments above. For compounds bearing 6-OMe substituents (**4**, **5**, **6**, and **8**), the Ar−Ar′ rotation experiences considerable hindrance as calculated and observed in the increased energy barrier range of $\Delta G^{\ddagger}$ = 123.0−135.6 kJ/mol, comparable to that observed for compound **13** (Figure 5a).

The transition state of **1** (Figure 6b) depicts that the Ar−CO rotation is facilitated by the presence of a twisted out-of-plane biaryl, which provides space for amide carbonyl rotation without interference. Thus, for 3-unsubstituted biaryls **1** and **3**−**6**, calculations of the Ar−CO bond rotation gave a range $\Delta G^{\ddagger}$ = 60.5−68.9 kJ/mol, resembling the observed Ar−CO bond rotation barrier of **16** (Figure 5c). For naphthamide **2**, exhibiting a *peri*-H interaction, and biaryl amides **7** and **8** experiencing rotational hindrance from the 3-methyl group, it was not possible to locate a transition state for the Ar−CO rotation. Instead, a transition state was located that shows the NEt_2 group rotated away from the otherwise favored planar amide structure. This, in turn, corresponds to a concerted Ar−CO/Et_2N−CO rotation transition state (similar to those depicted in Figures 6c,f), which could also be located for all other structures. This concerted rotation was also visible in the EXSY-NMR experiments of **8** where a faster Et_2N−CO rotation ($\Delta G^{\ddagger}_{EXSY}$ = 98.0 kJ/mol)) (SI, section 2.2) was observed together with the concerted rotation (entry 9, Table 2) by the individual amide ethyl-2′-CH_3 signals.

The concerted rotation may be represented by two transition states, with either the C═O or the Et_2N group oriented toward the Ar′ ring (i.e., Ar′ and O or Ar′ and N eclipsed as depicted in parts c and f, respectively, of Figure 6). Both transition states have very similar energies ($\Delta\Delta G$ < 4 kJ/mol), and only compounds **2**, **6**, and **8** exhibit a preference for the Ar′−N-type transition state, most likely due to increased steric bulk from the 6-substituent.

Consideration of the possible atropdiasteromers (Figure 4) in the context of the VT-NMR results suggests that either the Ar−Ar′ or the Ar−CO rotation is observed depending on which process has the lowest rotational barrier. On average, our calculations overestimate the experimentally measured values by ∼3.8 kJ/mol, with the largest deviation being 5.4 kJ/mol for compounds **1**, **5**, and **8**. However, due to the consistency of overestimation, the predicted barriers still correlate quite well with the experimental data.

Atropdiastereomer **8**, which displays both Ar−Ar′ and Ar−CO hindered rotations, shows an energy barrier of $\Delta G^{\ddagger}$ = 102.6 kJ/mol by EXSY-NMR (entry 9, Table 2), which is in good agreement with kinetic measurements for the atropisomerization of **8B** to **8A**/**B** by ^{1}H NMR, which gave $\Delta G^{\ddagger}$ = 103.8 kJ/mol (entry 10, Table 2). DFT computation of concerted Ar−CO and C−N bond rotations for compound **8** gave $\Delta G^{\ddagger}$ = 108.1 kJ/mol, in reasonable agreement with the experimental result. In contrast, the Ar−Ar′ rotation provided $\Delta G^{\ddagger}$ = 126.7 kJ/mol. For a comparison, concerted Ar−CO and C−N bond rotations reported by Clayden on *N*-(2,5-pyrrolidin-1-yl)-2-methylnaphthalene-1-amide show a $\Delta G^{\ddagger} \approx$ 104 kJ/mol.[31]

MECHANISTIC IMPLICATIONS

In order to enhance mechanistic understanding of the directed remote metalation (DreM) reaction,[32] biaryls with DMG = 2-COOH[33] and DMG = 2-$CONEt_2$[34] have been investigated for which a CIPE-induced mechanism has been implicated.[15c] The DreM reaction of 2-*N*,*N*-diethylcarbamoyl-2′-methyl biaryls which undergo 2′-methyl deprotonation and cyclization to phenanthrenes has seen extensive use in synthesis.[15,32] For this series as well, the DreM reaction has been postulated to occur by initial coordination of the alkyllithium or lithium dialkylamide base to the amide carbonyl (CIPE[15c]), followed by 2′-Me deprotonation and attack of the resulting tolyl anion on the 2-amide C═O bond followed by aromatization to the corresponding 9-phenanthrol derivative. In the present study, we observed that the biaryl amides, all bearing 2′-methyl groups, may be categorized in two series: compounds **1**, **2**, **4**, **5**, **7**, and **8** which undergo formation to phenanthrol derivatives[16] (e.g., **9**, Scheme 1) and compounds **3** and **6**[16] which afford fluorenones (e.g., **10**). The favorable DMG effect of the fluoro substituent in **6** is evident in the regioselective formation of the corresponding fluorenone[17] and in other cases.[35]

Based on a considerable body of studies,[36] nucleophilic reactions on amides involves an initial nucleophilic attack on the carbonyl to form a tetrahedral intermediate. In our systems, this demands that the biaryl *o*-amide adopt a rotational position in the transition state in accord with the Bürgi−Dunitz postulate[37] which states that, in the trajectory of approach empirically developed from a large body of X-ray structures, a nucleophile−C−O bond angle of 100−110° (modified to 93−102° for O- and N-nucleophiles by Cieplak[38]) is achieved in the last 2−3 Å before bond formation. Thus, as shown in Figure 7,

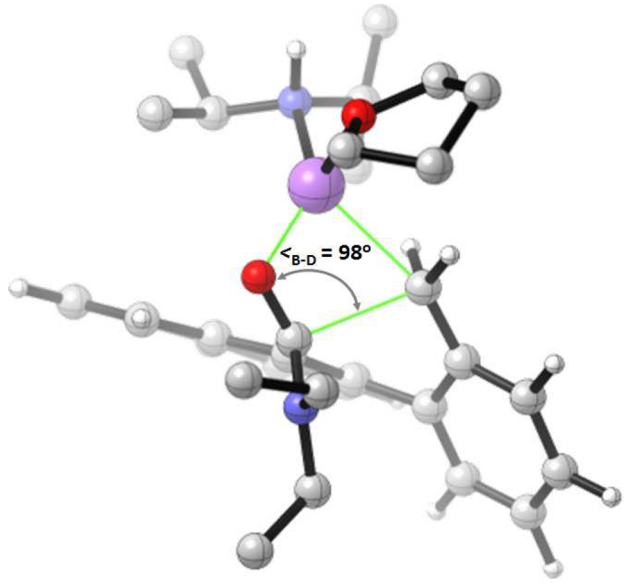

Figure 7. Computed transition state for the formation of the tetrahedral intermediate from 2′-methyl anion approach to the recipient C═O of **3** along the Bürgi−Dunitz angle. Hydrogen atoms of the THF and iPr$_2$NH ligands and of the ethyl groups of the amide have been omitted for clarity.

the amide group must undergo rotation orienting the NR_2 group partly over the biaryl system while the Ar−Ar′ bond undergoes concurrent rotation into a position for the tolyl carbanion to attack the carbonyl to achieve ring closure.

X-ray crystallographic studies of *ortho*-lithiated *N*,*N*-diisopropylbenzamide and *N*,*N*-diisopropylnaphthamide have shown dimeric structures with amide−aryl bond angles of 47° and 65° respectively,[39,40] indicating that, in the solid state, planarity of Li−C═O interaction is achieved to higher degree than the unmetalated systems (amide-Ar ring bond angle =

DOI: 10.1021/acs.joc.7b00890
J. Org. Chem. 2017, 82, 7300−7308

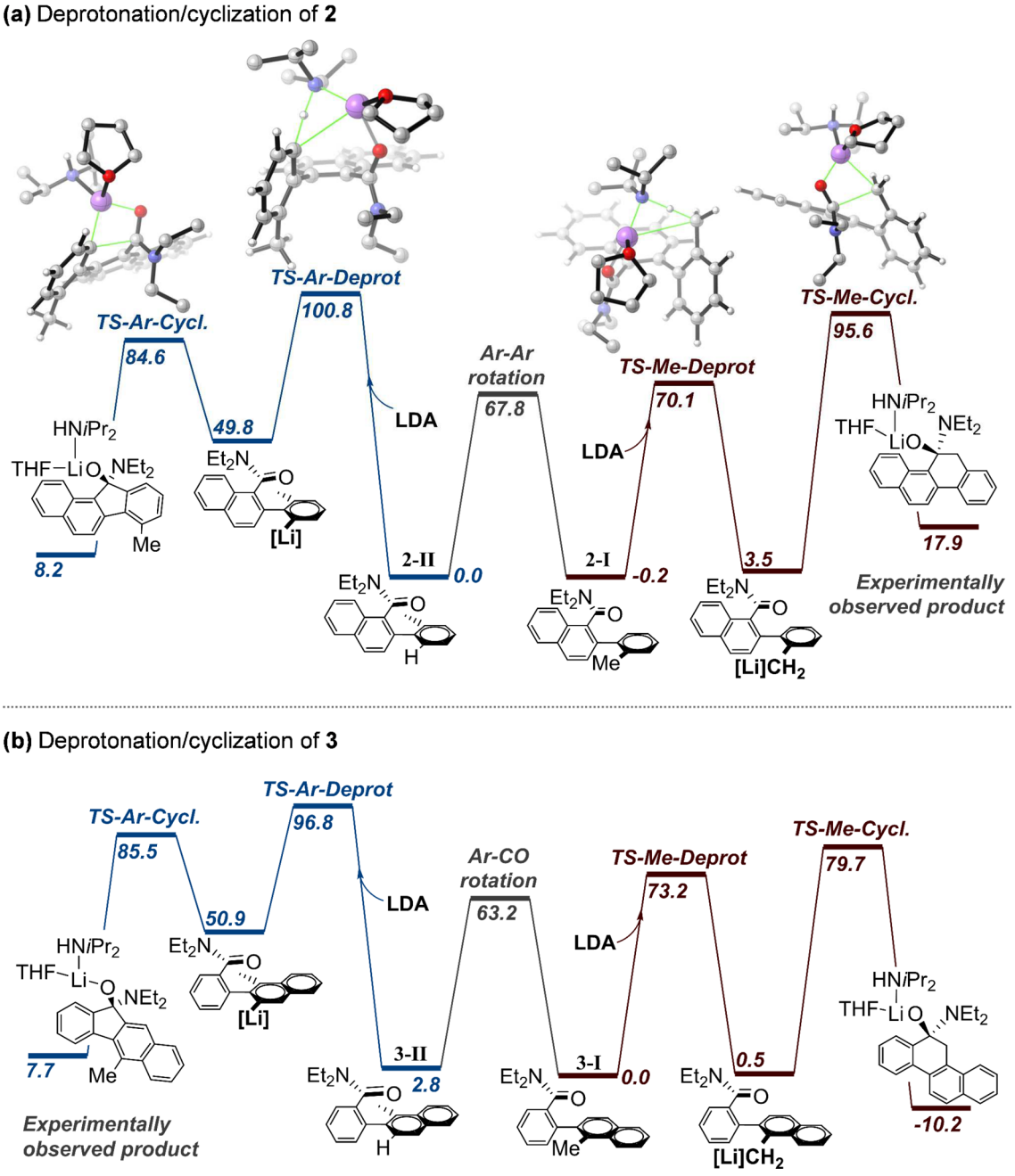

Figure 8. Comparison of the free energy (in kJ/mol) pathways of 2′-Me and Ar′ ring-deprotonation and the consecutive cyclization reactions of **2** (top) and **3** (bottom). Hydrogen atoms of the THF and iPr$_2$NH ligands and of the ethyl groups of the amide have been omitted for clarity. [Li] = −Li(iPr$_2$NH)(THF).[42]

90°). Recent studies of laterally metalated *N,N*-diisopropyl 2-propylbenzamide in solution reveal similar structures in which Li is coordinated to both carbonyl and the anion, to the extent that tridentate amine and ether ligands PMDTA (*N,N,N′,N″,N″*-pentamethyldiethylenetriamine) and DGME (diglyme) prefer dicoordination to the tetra-coordinating Li, leaving one amine free in solution.[41] With these mechanistic considerations in mind, a computational study was conducted for the proposed pathways of the DreM reaction of **2** and **3** with LDA (Figure 8).[42] The coordination sphere of Li was saturated with an explicitly included molecule of THF.[43] The calculated mechanism included an initial endergonic precomplexation of LDA with the biaryl, followed by deprotonation of either the Ar′-H or the 2′-Me position and subsequent nucleophilic attack of the resulting lithiated position on the amide carbonyl, resulting in ring closure and eventual formation of either the fluorenone **10** or the phenanthrol **11** derivatives, respectively. Bond lengths and angles in the coordination sphere of Li were quite similar to those obtained from X-ray structures by Wheatley.[39−41] For both substrates **2** and **3**, the metalation of the 2′-methyl group was found to be kinetically and thermodynamically favored over Ar′-metalation ($\Delta\Delta G^{\ddagger}$ = 24−31 kJ/mol). The Ar′ metalation was found to be endergonic by ∼50 kJ/mol, while the 2′-Me deprotonation was nearly thermoneutral (ΔG < 4 kJ/mol). With a concerted rotation of Ar−Ar′, Ar−CO, and Et$_2$N−CO bonds, both **2** and **3** show the ability to attain transition states complying with the Bürgi−Dunitz angle (Figure 7) (fluorenone: 107°, phenanthrol:

DOI: 10.1021/acs.joc.7b00890
J. Org. Chem. 2017, 82, 7300−7308

98−99°). For Ar′ ring deprotonation−cyclization to the fluorenone (Figure 8), these transition states were found to be lower in energy than the preceding deprotonation step; for 2′-Me-deprotonation−cyclization to the phenanthrols, they were higher in energy. However, since the transition states for the cyclization for both substrates **2** and **3** have lower barriers than the highest transition states in the Ar′-deprotonation−cyclization pathway ($\Delta\Delta G^{\ddagger}$ = 8−13 kJ/mol in favor of the fluorenone formation pathway), these calculations are not in full agreement with the different outcomes of the reactions of **2** and **3**. In fact, from the calculated model, the formation of the phenanthrol **11** from **3** is both thermodynamically and kinetically more favorable than the formation of **9** from **2**, which is opposite to experimental observations. Thus, the considered reaction mechanism and the employed computational results suggest that both of the substrates should favor 2′-Me deprotonation and a subsequent ring closure to a phenanthrol derivative. Whether there is involvement of dimers, multiple metalations (sometimes 2 equiv or more of organolithium base is needed for DreM reactions), or different complexation from those based on the CIPE concept[15c] are current speculations for further investigations.

CONCLUSIONS

Based on VT ^{1}H NMR measurements, EXSY-NMR experiments, and computational studies, we conclude that 2-amido-2′-methyl biphenyls **1**−**8** may be described as atropdiastereomers involved in dynamic bond rotation around the Ar−Ar′ and Ar−CO bonds, which is dependent on the location of substituents. For biaryls bearing a substituent *ortho* to the amide functional group (**2**, **7**) in which the Ar−CO rotation is hindered, the Ar−Ar′ rotation shows the lower energy barrier ($\Delta G^{\ddagger}_{Tc}$ = 64.8−67.5 kJ/mol), while compounds with substituents located *ortho* to the biaryl bond (**4**−**6**), which hinder this rotation, show lower energy barriers for the Ar−CO rotation ($\Delta G^{\ddagger}_{Tc}$ = 60.5−63.0 kJ/mol). For 2-amido-2′-methyl biaryls bearing a substituent *ortho* to both the amide and the biaryl bond (**8**), true isolable atropisomers were observed at room temperature, and the measured energy barrier for atropdioastereomeric interconversion ($\Delta G^{\ddagger}$ = 102.6−103.8 kJ/mol) complied with a concerted Ar−CO/Et$_2$N−CO bond rotation. Neither calculated nor measured rotational barriers were sufficiently high to interfere with or allow rationalization of the different reactivity of these compounds in the cyclization to fluorenones or phenathrols by the directed remote metalation (DreM) reaction.

EXPERIMENTAL SECTION

General Methods. Tetrahydrofuran (THF) was distilled under nitrogen atmosphere from Na/benzophenone. *N*,*N*,*N*′,*N*′-Tetramethylethylenediamine (TMEDA) was distilled and stored over potassium hydroxide (KOH). A glove box was used when necessary. All reactions were carried out under nitrogen atmosphere if not otherwise specified. TLC was performed on Merck silica gel 60 F_{254} plates using UV light at 254 nm and 5% alcoholic molybdophosphoric acid for detection. Normalsil 60, 40−63 μm silica gel, was used for flash chromatography. ^{1}H and ^{13}C NMR were recorded on a Varian Mercury 300 MHz (UiS, Norway) or a Bruker AVANCE 400 (automatic sample changer, BB auto tuning; Queen's University, Kingston, ON, Canada), all at room temperature. Chloroform-d_1 was used as solvent unless otherwise specified. Chemical shift was reported in ppm compared to TMS (δ 0, singlet, for ^{1}H NMR) or for ^{13}C resonance signal to $CDCl_3$ (δ 77.0, triplet). The splitting pattern was recorded as a singlet, s; doublet, d; triplet, t; double doublet, dd; double triplet, dt; quartet, q; multiplet, m; broad, br. IR was recorded on a PerkinElmer FT-IR spectrometer, version 3.02.01. HRMS was measured on a LTQ Orbitrap XL ion trap mass spectrometer with electrospray ionization. Melting points was determined on a Stuart Scientific melting point apparatus SMP3 and are uncorrected. Syntheses of compounds **1** and **4**−**8** were reported previously.[16]

*N,N-Diethyl-2-(o-tolyl)-1-naphthamide (**2**).* *N*,*N*-Diethyl-1-naphthoylamide (0.781 g, 3.44 mmol) in THF (10 mL) was added dropwise to a solution of *s*-BuLi (3.7 mL, 5.17 mmol, 1.4 M solution in cyclohexane) and TMEDA (0.77 mL, 5.16 mmol) in THF (10 mL) at −78 °C. After the solution was stirred for 1 h, triisopropyl borate (1.97 mL, 8.59 mmol) was added, and the mixture stirred at −78 °C for 1.5 h and warmed to rt over 18 h. The reaction mixture was quenched with NH_4Cl (15 mL) and extracted with diethyl ether (3 × 15 mL). The organic layer was washed with water (2 × 45 mL), dried over $MgSO_4$, subjected to filtration, and concentrated in vacuo to give 1-(diethylcarbamoyl)naphthalene-2-yl)boronic acid as a brown oil which was used without further purification in the next experiment.

All solutions were degassed prior to use. A mixture of $PdCl_2$(dppf) (118 mg, 0.14 mmol, 5 mol %) and 2-bromotoluene (0.35 mL, 2.91 mmol) in DME (6 mL) was stirred at room temperature for 15 min. The solution of (1-(diethylcarbamoyl)naphthalen-2-yl)boronic acid (3.44 mmol) in DME (4 mL) was added, followed by 2 M Na_2CO_3 (6 mL), at room temperature. The mixture was heated at reflux for 18 h, cooled, and extracted with diethyl ether (3 × 20 mL). The organic layer was dried over $MgSO_4$, subjected to filtration, and concentrated in vacuo. The crude product was purified by flash column chromatography (petroleum ether/ethyl acetate 2:1) to afford 0.85 g (92%) of **2** as a brown oil as a ca. 3:2 mixture of rotamers. ^{1}H NMR ($CDCl_3$, 300 MHz): δ 7.87−7.85 (app m, 3H), 7.57−7.51 (m, 3H), 7.42−7.13 (m, 4H), 3.89−3.82 (m, 1H), 3.26−2.70 (m, 3H), 2.26 and 2.19 (s, 3H), 0.94−0.70 (m, 6H). ^{13}C NMR ($CDCl_3$, 75 MHz): δ 168.9 (CO), 139.9 (*C*), 138.6 (*C*), 137.8 (*C*), 134.9 (*C*), 133.9 (*C*), 132.5 (CH), 131.2 (CH), 130.0 (04) (CH), 130.0 (0) (CH), 128.2 (CH), 128.1 (CH), 128.0 (CH), 127.7 (CH × 2), 127.5 (CH), 126.9 (CH × 2), 126.2 (CH), 125.6 (CH), 125.5 (*C* × 2), 124.5 (*C* × 2), 42.7 (NCH_2 - minor rotamer), 42.1 (NCH_2 - major rotamer), 37.7 (NCH_2 - major rotamer), 37.5 (NCH_2 - minor rotamer), 20.4 (CH_3 - minor rotamer), 20.3 (CH_3 - major rotamer), 13.9 (2) (NCH_2CH_3 - minor rotamer), 13.9 (0) (NCH_2CH_3 - major rotamer), 11.9 (NCH_2CH_3 - major rotamer), 11.6 (NCH_2CH_3 - minor rotamer). IR (KBr): 3055 (w), 2974 (m), 2933 (m), 2873 (w), 2238 (w), 1628 (s), 1492 (m), 1473 (m), 1434 (s), 1381 (m), 1280 (m), 1267 (m), 1221 (m), 1128 (m), 828 (m), 761 (m), 728 (m). Mass spectrum *m*/*z* (relative intensity): 340.2 $[M + Na]^+$ (100). HRMS (ESI): calcd for $C_{22}H_{23}ON$ + Na 340.1672, found 340.1671.

*N,N-Diethyl-2-(1-methylnaphthalen-2-yl)benzamide (**3**).* *N*,*N*-Diethylbenzamide (612 mg, 3.45 mmol) in THF (10 mL) was added dropwise to a solution of *s*-BuLi (3.7 mL, 5.18 mmol, 1.4 M solution in cyclohexane), TMEDA (0.77 mL, 5.16 mmol), and THF (10 mL) at −78 °C. After the solution was stirred for 1 h, triisopropyl borate (1.97 mL, 8.59 mmol) was added, and the mixture was stirred at −78 °C for 1.5 h and warmed to rt over 18 h. The reaction mixture was quenched with NH_4Cl solution (15 mL) and extracted with diethyl ether (3 × 15 mL). The organic layer was washed with water (2 × 45 mL), dried over $MgSO_4$, subjected to filtration, and concentrated in vacuo to give 2-(*N*,*N*-diethylcarboxamido)phenylboronic acid as a brown oil which was used without further purification in the next experiment.

All solutions were degassed prior to use. A mixture of $PdCl_2$(dppf) (116 mg, 0.14 mmol, 5 mol %) and 2-bromo-1-methylnaphthalene (638 mg, 2.89 mmol) in DME (6 mL) was stirred at room temperature for 15 min under inert atmosphere. The solution 2-(*N*,*N*-diethylcarboxamido)phenylboronic acid (3.45 mmol) in DME (4 mL) followed by 2 M Na_2CO_3-solution (6 mL) was added at room temperature, and the mixture was heated at reflux for 18 h. After the mixture was allowed to cool it was extracted with diethyl ether (3 × 20 mL). The organic layer was dried over $MgSO_4$, subjected to filtration, and concentrated in vacuo. The crude product was purified by flash chromatography (petroleum ether/ethyl acetate 2:1) to afford 862 mg (94%) of product **3** as a viscous, brown/red oil. ^{1}H NMR ($CDCl_3$, 300

DOI: 10.1021/acs.joc.7b00890
J. Org. Chem. 2017, 82, 7300−7308

MHz): δ 8.02 (app s, 1H), 7.78 (app s, 1H), 7.50−7.30 (m, 8H), 3.58−2.35 (5 peaks app s, 4H), 2.71 (s, 3H), 1.28−1.11 (m, 3H), 0.60−0.5 (m, 3H). ^{13}C NMR ($CDCl_3$, 75 MHz): δ 170.0 (*C*O), 137.2 (*C*), 134.2 (*C*), 131.5 (*C*), 129.0 (*C*H), 128.3 (*C*H × 2), 127.8 (*C*), 127.6 (*C*H × 2), 126.9 (*C*), 126.2 (*C*H × 2), 125.8 (*C*H), 125.5 (*C*H × 2), 124.6 (*C*). IR (KBr): 3064 (w), 2973 (m), 2933 (m), 2872 (w), 1630 (s), 1513 (w), 1458 (m), 1426 (m), 1381 (m), 1288 (m), 1221 (w), 1098 (m), 1078 (w), 871 (w), 836 (w), 784 (w), 764 (m), 480 (m), 471 (m). Mass spectrum *m*/*z* (relative intensity): 340.2 $[M + Na]^+$ (74). HRMS (ESI): cald for $C_{22}H_{23}NO$ + Na 340.16789, found 340.16773.

Variable-Temperature NMR. Variable-temperature NMR (VT NMR) were carried out with temperatures ranging from 190 K (−83 °C) to 332 K (59 °C). All compounds were recorded on a 400 MHz Bruker NMR using toluene-d_8 as solvent. The temperature of the probe used in these experiments was calibrated by an ethylene glycol solution. From $\Delta\upsilon$, the rate constant, k_c (the rate for rotamer interconversions) at coalescence temperature, T_c, was calculated by the Gutowsky−Holm equation ($k_c = \pi\Delta\upsilon/\sqrt{2} = \sim 2.22\Delta\upsilon$ s^{-1}).[44] The temperature was raised from a temperature sufficiently low to observe separate signals for the tolyl methyl group until the coalescence of the two peaks was reached. From the coalescence temperature, T_c, and the rate constant, k_c, the activation energy of rotation ($\Delta G^{\ddagger}_{Tc}$) was calculated using the Eyring equation ($\Delta G^{\ddagger}_{Tc} = RT_c[23.76 - \ln(k_c/T_c)]$), where *R* is the gas constant, 8.3145 kJ/mol.[45] The margin of error was estimated to ±0.8 kJ/mol by estimating the accuracy of $\Delta\upsilon$ and T_c from the measurements and applying the extremities in the calculations.

Spectra of the variable-temperature experiments of compounds **1**−**7** are given in the SI, section 1, together with a more comprehensive description. The rotational barriers for compound **8** could not be measured as the coalescence temperature was not reached at 380 K, which was the limit of the NMR probe.

EXSY NMR Experiments. The EXSY experiments[46] were performed on a Bruker AVANCE 600 spectrometer using the standard noesygpph pulse program. The spectra window was set to 8 ppm, and 2K × 512 data points were acquired and zero-filled to 2K × 2K. Different mixing times were performed from 0.001 s up to 80% of the relaxation time of the appropriate nuclei. The mixing time was changed to obtain EXSY spectra that contained no exchange between peaks and compare it with EXSY spectra that contained exhange between peaks. Integration of diagonal and cross peaks and comparison with the two mixing times provided the rate of the isomeric interconversion. From the rate of interconversion *k* at a given temperature *T*, the rotational energy barrier was then calculated ($\Delta G^{\ddagger} = RT[23.76 - \ln(k/T)]$). The data were processed using MestReNova, and the integration of the various signals was analyzed using the EXSYCalc program from MestReC to obtain the rate constant.[47]

EXSY NMR of 8. While the coalescence of the two isomeric 2′-methyl peaks of **8** was not observed in toluene-d_8, DMSO-d_6, or acetone-d_6, the rotational barrier could be measured from the volume integration of the exchanging peaks in an EXSY experiment by varying the mixing time from 1 to 0.01 s at 380 K.[48] At 1 s, the exchange between the protons could be observed, while at mixing time 0.01 s, no exchange was observed. By volume integration of the exchanging peaks, the rate of interconversion and the rotational energy barrier were calculated. In this EXSY experiment, two interconversions were observed: (a) the atropdiastereomeric **A**−**B** interconversion from the exchanging peaks of aromatic protons ($\Delta G^{\ddagger}_{EXSY}$ = 102.6 kJ/mol) and (b) the *syn*/*anti* Et_2N−CO **A**−**A**′ amide interconversion from the peaks representing the CH_3-amide proton exchange ($\Delta G^{\ddagger}_{EXSY}$ = 98.0 kJ/mol).

NMR spectra and a more comprehensive discussion of these experiments are given in the SI, section 2.

■ ASSOCIATED CONTENT

Supporting Information

The Supporting Information is available free of charge on the ACS Publications website at DOI: 10.1021/acs.joc.7b00890.

NMR spectra of new compounds, detailed discussion, spectra of VT and EXSY NMR experiments, and DFT calculations (PDF)

■ AUTHOR INFORMATION

Corresponding Authors

*E-mail: kare.b.jorgensen@uis.no.

*E-mail: snieckus@chem.queensu.ca.

ORCID

Victor Snieckus: 0000-0002-6448-9832

Notes

The authors declare no competing financial interest.

■ ACKNOWLEDGMENTS

We thank the High Performance Computing Virtual Laboratory (HPCVL), WestGrid High Performance Computing Consortium, and Professor Nicholas J. Mosey, Queen's University, for computing facilities. Part of the work was carried out in the University of Tartu High Performance Computing Centre. Support of the synthetic work by an NSERC Canada Discovery Grant (DG) is gratefully acknowledged.

■ REFERENCES

(1) Christie, G. H.; Kenner, J. H. *J. Chem. Soc., Trans.* **1922**, *121*, 614−620.

(2) Alkorta, I.; Elguero, J.; Roussel, C.; Vanthuyne, N.; Piras, P. In *Advances in Heterocyclic Chemistry*; Katritzky, A., Ed.; Academic Press, 2012; Vol. *105*, pp 1−188.

(3) (a) Peck, T. G.; Lai, Y. H. *Tetrahedron* **2009**, *65*, 3664−3667. (b) Mazzanti, A.; Lunazzi, L.; Minzoni, M.; Anderson, J. E. *J. Org. Chem.* **2006**, *71*, 5474−5481. (c) Leroux, F. *ChemBioChem* **2004**, *5*, 644−649. (d) Ceccacci, F.; Mancini, G.; Mencarelli, P.; Villani, C. *Tetrahedron: Asymmetry* **2003**, *14*, 3117−3122.

(4) (a) Brunel, J. M. *Chem. Rev.* **2005**, *105*, 857−897. (b) Meca, L.; Reha, D.; Havlas, Z. *J. Org. Chem.* **2003**, *68*, 5677−5680.

(5) (a) Kumarasamy, E.; Raghunathan, R.; Sibi, M. P.; Sivaguru, J. *Chem. Rev.* **2015**, *115* (20), 11239−11300. (b) Bringmann, G.; Mortimer, A. J. P.; Keller, P. A.; Gresser, M. J.; Garner, J.; Breuning, M. *Angew. Chem., Int. Ed.* **2005**, *44*, 5384−5427. (c) Berthod, M.; Mignani, G.; Woodward, G.; Lemaire, M. *Chem. Rev.* **2005**, *105*, 1801−1836. (d) Pu, L. *Chem. Rev.* **1998**, *98*, 2405−2494.

(6) (a) Smyth, J. E.; Butler, N. M.; Keller, P. A. *Nat. Prod. Rep.* **2015**, *32*, 1562−1583. (b) Bringmann, G.; Gulder, T.; Gulder, T. A. M.; Breuning, M. *Chem. Rev.* **2011**, *111*, 563−639. (c) Lloyd-Williams, P.; Giralt, E. *Chem. Soc. Rev.* **2001**, *30*, 145−157. (d) Williams, D. H.; Bardsley, B. *Angew. Chem., Int. Ed.* **1999**, *38*, 1172−1193. (e) Nicolaou, K. C.; Boddy, C. N. C.; Bräse, S.; Winssinger, N. *Angew. Chem., Int. Ed.* **1999**, *38*, 2096−2152. (f) Torssell, K. B. G. *Natural Product Chemistry*; Taylor and Francis: New York, 1997.

(7) (a) Zask, A.; Murphy, J.; Ellestad, G. A. *Chirality* **2013**, *25*, 265−274. (b) LaPlante, S. R.; Fader, L. D.; Fandrick, K. R.; Fandrick, D. R.; Hucke, O.; Kemper, R.; Miller, S. P. F.; Edwards, P. J. *J. Med. Chem.* **2011**, *54*, 7005−7022. (c) Laplante, S. R.; Edwards, P. J.; Fader, L. D.; Jakalian, A.; Hucke, O. *ChemMedChem* **2011**, *6*, 505−513. (d) Clayden, J.; Moran, W. J.; Edwards, P. J.; Laplante, S. R. *Angew. Chem., Int. Ed.* **2009**, *48*, 6398−6401.

(8) (a) Tietze, L. F.; Schuster, H. J.; von Hof, J. M.; Hampel, S. M.; Colunga, J. F.; John, M. *Chem. - Eur. J.* **2010**, *16*, 12678−12682. (b) Clayden, J. *Chem. Commun.* **2004**, 127−135. (c) Bowles, P.; Clayden, J.; Helliwell, M.; McCarthy, C.; Tomkinson, M.; Westlund,

DOI: 10.1021/acs.joc.7b00890
J. Org. Chem. 2017, 82, 7300−7308

N. *J. Chem. Soc., Perkin Trans. 1* **1997**, 2607−2616. (d) Clayden, J. *Angew. Chem., Int. Ed. Engl.* **1997**, *36*, 949−951 and references cited therein. (e) Cuyegkeng, M. A.; Mannschreck, A. *Chem. Ber.* **1987**, *120*, 803−809. (f) Ackerman, J. H.; Laidlaw, G. M.; Snyder, G. A. *Tetrahedron Lett.* **1969**, *10*, 3879−3882.

(9) (a) Berthelot-Bréhier, A.; Panossian, A.; Colobert, F.; Leroux, F. R. *Org. Chem. Front.* **2015**, *2*, 634−644. (b) Clayden, J.; Worrall, C. P.; Moran, W. J.; Helliwell, M. *Angew. Chem., Int. Ed.* **2008**, *47*, 3234−3237. (c) Koide, H.; Hata, T.; Uemura, M. *J. Org. Chem.* **2002**, *67*, 1929−1935. (d) Thayumanavan, S.; Beak, P.; Curran, D. P. *Tetrahedron Lett.* **1996**, *37*, 2899−2902.

(10) (a) Clayden, J.; Lai, L. W.; Helliwell, M. *Tetrahedron* **2004**, *60*, 4399−4412 and references cited therein. (b) Rios, R.; Jimeno, C.; Carroll, P. J.; Walsh, P. J. *J. Am. Chem. Soc.* **2002**, *124*, 10272−10273. (c) Dai, W. M.; Lau, C. W. *Tetrahedron Lett.* **2001**, *42*, 2541−2544.

(11) (a) Dai, W. M.; Yeung, K. K. Y.; Chow, C. W.; Williams, I. D. *Tetrahedron: Asymmetry* **2001**, *12*, 1603−1613. (b) Clayden, J.; Johnson, P.; Pink, J. H.; Helliwell, M. *J. Org. Chem.* **2000**, *65*, 7033−7040.

(12) (a) Meyers, A. I.; Nelson, T. D.; Moorlag, H.; Rawson, D. J.; Meier, A. *Tetrahedron* **2004**, *60*, 4459−4473. (b) Clayden, J.; McCarthy, C.; Cumming, J. G. *Tetrahedron Lett.* **2000**, *41*, 3279−3283.

(13) (a) Wiberg, K. B. In *The Amide Linkage: Structural Significance in Chemistry, Biochemistry, and Materials Science*; Greenberg, A., Breneman, C. M., Liebman, J. F., Eds.; Wiley: New York, 2003; pp 33−46. (b) Scherer, G.; Kramer, M. L.; Schutkowski, M.; Reimer, U.; Fischer, G. *J. Am. Chem. Soc.* **1998**, *120*, 5568−5574. (c) Stewart, W. E.; Siddall, T. H. *Chem. Rev.* **1970**, *70*, 517−551.

(14) (a) Bragg, R. A.; Clayden, J.; Morris, G. A.; Pink, J. H. *Chem. - Eur. J.* **2002**, *8*, 1279−1289. (b) Clayden, J.; Frampton, C. S.; McCarthy, C.; Westlund, N. *Tetrahedron* **1999**, *55*, 14161−14184. (c) Clayden, J.; McCarthy, C.; Helliwell, M. *Chem. Commun.* **1999**, 2059−2060. (d) Clayden, J. *Synlett* **1998**, *1998*, 810−816. (e) Ahmed, A.; Bragg, R. A.; Clayden, J.; Lai, L. W.; McCarthy, C.; Pink, J. H.; Westlund, N.; Yasin, S. A. *Tetrahedron* **1998**, *54*, 13277−13294.

(15) (a) Wang, X.; Fu, J.-m.; Snieckus, V. *Helv. Chim. Acta* **2012**, *95*, 2680. (b) Snieckus, V.; Macklin, T. In *Handbook of C−H Transformations*; Dyker, G., Ed.; Wiley-VCH: Weinheim, 2005; Vol. *1*, p 106. (c) Whisler, M. C.; MacNeil, S.; Snieckus, V.; Beak, P. *Angew. Chem., Int. Ed.* **2004**, *43*, 2206−2225. (d) Fu, J. M.; Snieckus, V. *Can. J. Chem.* **2000**, *78*, 905.

(16) Jørgensen, K. B.; Rantanen, T.; Dörfler, T.; Snieckus, V. *J. Org. Chem.* **2015**, *80*, 9410−9424.

(17) Beak has shown that directed *ortho* metalation in amides is dependent on the dihedral angle between the hydrogen abstracted and the proximate amide carbonyl. Our biaryl cases deal with very different geometry considerations in remote metalation of aryl C−H and C−CH_3 deprotonations: Beak, P.; Kerrick, S. T.; Gallagher, D. J. *J. Am. Chem. Soc.* **1993**, *115*, 10628−10636.

(18) Mohri, S.-I.; Stefinovic, M.; Snieckus, V. *J. Org. Chem.* **1997**, *62*, 7072−7073.

(19) (a) Friebolin, H. *Basic One- and Two-Dimensional NMR spectroscopy*, 3rd ed.; Wiley: Weinheim, 1998; Chapter 11. (b) Günther, H. *NMR Spectroscopy − Basic Principles, Concepts, And Applications in Chemistry*, 2nd ed.; Wiley: New York, 1995; Chapter 9. (c) Allerhand, A.; Gutowsky, H. S.; Jonas, J.; Meinzer, R. A. *J. Am. Chem. Soc.* **1966**, *88*, 3185−3194.

(20) Kincaid, J. F.; Eyring, H.; Stearn, A. E. *Chem. Rev.* **1941**, *28*, 301.

(21) The available NMR probe could not safely achieve a higher temperature.

(22) Meier, B. H.; Ernst, R. R. *J. Am. Chem. Soc.* **1979**, *101*, 6441.

(23) Förster, H.; Vögtle, F. *Angew. Chem., Int. Ed. Engl.* **1977**, *16*, 429−441.

(24) Baker, R. W.; Brkic, Z.; Sargent, M. V.; Skelton, B. W.; White, A. H. *Aust. J. Chem.* **2000**, *53*, 925−938.

(25) Berg, U.; Bladh, H. *Acta Chem. Scand.* **1998**, *52*, 1380−1385.

(26) Wolf, C.; Hochmuth, D. H.; König, W. A.; Roussel, C. *Liebigs Ann.* **1996**, *1996*, 357−363.

(27) Bott, G.; Field, L. D.; Sternhell, S. *J. Am. Chem. Soc.* **1980**, *102*, 5618−5626.

(28) (a) Frisch, M. J.; et al. *Gaussian 09*, revision A.02; Gaussian, Inc.: Wallingford, 2009. (See the SI for the full reference.) (b) While the M06-2X functional has been successfully employed in the computational prediction of rotation barriers (see ref 28c), we observed that in our case it yielded ∼4 kJ/mol higher barriers for the Ar−Ar and Ar−CO rotations and ∼4 kJ/mol lower barriers for the C−N and combined rotations than the M06L functional.. (c) Jackson, K. E.; Mortimer, C. L.; Odell, B.; McKenna, J. M.; Claridge, T. D. W.; Paton, R. S.; Hodgson, D. M. *J. Org. Chem.* **2015**, *80*, 9838−9846.

(29) Two possible transition states were considered where either the carbonyl or the NR_2 group of the amide is toward the *o*-aryl substituent. (See the SI for details.)

(30) (a) Clayden, J.; Lund, A.; Vallverdú, L.; Helliwell, M. *Nature* **2004**, *431*, 966−971. (b) Betson, M. S.; Bracegirdle, A.; Clayden, J.; Helliwell, M.; Lund, A.; Pickworth, M.; Snape, T. J.; Worrall, C. P. *Chem. Commun.* **2007**, 754−756.

(31) Clayden, J.; Pink, J. H. *Angew. Chem., Int. Ed.* **1998**, *37*, 1937−1939.

(32) Tilly, D.; Magolan, J.; Mortier, J. *Chem. - Eur. J.* **2012**, *18*, 3804−3820.

(33) (a) Castanet, A.-S.; Tilly, D.; Véron, J.-B.; Samanta, S. S.; De, A.; Ganguly, T.; Mortier, J. *Tetrahedron* **2008**, *64*, 3331−3336. (b) Tilly, D.; Samanta, S. S.; Castanet, A.-S.; De, A.; Mortier, J. *Eur. J. Org. Chem.* **2006**, *2006*, 174−182. (c) Tilly, D.; Samanta, S. S.; De, A.; Castanet, A.-S.; Mortier, J. *Org. Lett.* **2005**, *7* (5), 827−830.

(34) Tilly, D.; Fu, J.-M.; Zhao, B.-P.; Alessi, M.; Castanet, A.-S.; Snieckus, V.; Mortier, J. *Org. Lett.* **2010**, *12* (1), 68−71.

(35) Klís, T.; Lulínski, S.; Serwatowski, J. *Curr. Org. Chem.* **2008**, *12*, 1479−1501.

(36) McMurry, J. *Organic Chemistry*, 9th ed.; Cengage Learning, 2016; pp 710−711.

(37) Bürgi, H. B.; Dunitz, J. D.; Lehn, J. M.; Wipf, G. *Tetrahedron* **1974**, *30*, 1563−1572.

(38) Cieplak, A. S. *Organic Addition and Elimination Reactions; Transformation Paths of Carbonyl Derivatives in Structure Correlation*; Bürgi, H.-B., Dunitz, J. D., Eds.; VCH: Weinheim, 1994; Vol. *1*, pp 205−302 (pp 210−218).

(39) Clayden, J.; Davies, R. P.; Hendy, M. A.; Snaith, R.; Wheatley, A. E. H. *Angew. Chem., Int. Ed.* **2001**, *40*, 1238−1240.

(40) Armstrong, D. R.; Clayden, J.; Haigh, R.; Linton, D. J.; Schooler, P.; Wheatley, A. E. H. *Chem. Commun.* **2003**, 1694−1695.

(41) (a) Vincent, M. A.; Smith, A. C.; Donnard, M.; Harford, P. J.; Haywood, J.; Hillier, I. H.; Claydon, J.; Wheatley, A. E. H. *Chem. - Eur. J.* **2012**, *18*, 11036−11045. (b) Wheatley, A. E. H.; Clayden, J.; Hillier, I. H.; Smith, A. C.; Vincent, M. A.; Taylor, L. J.; Haywood, J. *Beilstein J. Org. Chem.* **2012**, *8*, 50−60.

(42) Calculations were performed at the CPCM (THF) M06L/6-311++G(d)//CPCM (THF) ωB97XD/6-31+G(d) level of theory.

(43) Various ligation states of Li were considered: only iPr$_2$NH base; two THF molecules; and a combination of one iPr$_2$NH and one THF molecule. The latter was found to be the most favored in all considered stages of the reaction.

(44) (a) Modarresi-Alam, A. R.; Amirazizi, A.; Bagheri, H.; Bijanzadeh, H. R.; Kleinpeter, E. *J. Org. Chem.* **2009**, *74*, 4740−4746. (b) Günther, H. *NMR spectroscopy − Basic principles, concepts, and applications in chemistry*, 2nd ed.; Wiley: New York, 1995; Chapter 9. (c) Friebolin, H. *Basic One- and Two-Dimensional NMR Spectroscopy*, 3rd ed.; Wiley: Weinheim, 1998; Chapter 11. (d) Yamagami, C.; Takao, N.; Takeuchi, Y. *Aust. J. Chem.* **1986**, *39*, 457−463.

(45) Kincaid, J. F.; Eyring, H.; Stearn, A. E. *Chem. Rev.* **1941**, *28*, 301.

(46) Meier, B. H.; Ernst, R. R. *J. Am. Chem. Soc.* **1979**, *101*, 6441.

(47) Cobas, J. C.; Pastorm, M. M. *EXSYCalc*, version 1.0; MestReC, 2004.

(48) (a) Zolnai, Z.; Juranic, N.; Vikic-Topic, D.; Macura, S. *J. Chem. Inf. Comput. Sci.* **2000**, *40*, 611−621. (b) Lu, J.; Ma, D.; Hu, J.; Tang, W.; Zhu, D. *J. Chem. Soc., Dalton Trans.* **1998**, 2267−2273.

DOI: 10.1021/acs.joc.7b00890
J. Org. Chem. 2017, 82, 7300−7308